Theor Chem Acc (2007) 117: 291–296
DOI 10.1007/s00214-006-0133-1

REGULAR ARTICLE

Maciej Harańczyk · Maciej Gutowski

Differences in electrostatic potential around DNA fragments containing guanine and 8-oxo-guanine

Received: 1 July 2005 / Accepted: 6 October 2005 / Published online: 26 September 2006

Abstract Changes of electrostatic potential (EP) around the DNA molecule resulting from chemical modifications of nucleotides may play a role in enzymatic recognition of damaged sites. Effects of chemical modifications of nucleotides on the structure of DNA have been characterized through large-scale density functional theory computations. Quantum mechanical structural optimizations of DNA fragments with three pairs of nucleotides and accompanying counteractions were performed with a B3LYP exchange-correlation functional and 6–31G** basis sets. The "intact" DNA fragment contained guanine in the middle layer, while the "damaged" fragment had the guanine replaced with 8-oxo-guanine. The electrostatic potential around these DNA fragments was projected on a surface around the double helix. The 2D maps of EP of intact and damaged DNA fragments were analyzed to identify these modifications of EP that result from the occurrence of 8-oxo-guanine. It was found that distortions of the phosphate groups and displacements of the accompanying countercations are clearly reflected in the EP maps.

Keywords DNA damage · 8-oxo-guanine · Electrostatic potential

Electronic supplementary material Supplementary material is available in the online version of this article at http://dx.doi.org/10.1007/s00214-006-0133-1 and is accessible for authorized users.

M. Harańczyk (✉) · M. Gutowski
Chemical Sciences Division,
Pacific Northwest National Laboratory,
Richland, WA 99352, USA
E-mail: maharan@chem.univ.gda.pl

M. Harańczyk
Department of Chemistry, University of Gdańsk,
Sobieskiego 18, 80-952 Gdańsk, Poland

M. Gutowski
Chemistry-School of Engineering and Physical Sciences,
Heriot-Watt University, William H Perkin Building,
Edinburgh EH14 4AS, UK
E-mail: m.gutowski@hw.ac.uk

1 Introduction

DNA in living cells is exposed continuously to a number of environmental agents, which include UV and ionizing radiation as well as various chemical species. In many cases, the mechanism of action of these agents involves generation of free radicals that attack DNA and produce a variety of lesions, including sugar and base modifications, strand breaks, and cross-links. Some active oxygen radicals (e.g., O_2^-, •OH) are also generated endogenously during cellular aerobic metabolism, and the damage they cause may be an important factor in aging and age-dependent diseases, including cancer [1–4].

The genomes of aerobic organisms suffer from chronic oxidation of guanine (G) to a genotoxic product 8-oxo-guanine (8oG) (Fig. 1) [5]. The replicative DNA polymerases misread 8oG residues and insert adenine instead of cytosine opposite to the oxidized base. Both bases in the resulting A-8oG mispair are mutagenic lesions, and both undergo base-specific replacements to restore the original C–G pair [6] . Doing so represents a formidable challenge to the DNA repair machinery, because adenine makes up roughly 25% of the bases in most genomes.

Nature has developed very efficient pathways for repairing sites containing 8oG. The enzymatic DNA damage detection and repair is a complex multi-step process. However, the idea of damage detection is fairly simple: the enzyme has to locate the damage based on features that make those sites different from intact fragments of DNA. The DNA–enzyme interaction is determined by three typical interactions in chemistry: hydrogen bonds, electrostatic interactions and dispersion forces. The first two have the same origin and result from the interaction of static charges while dispersion interaction can be associated with the interaction of instantaneous multipoles. In this work, we analyze electrostatic potential around an intact DNA fragment and around the same fragment but with guanine being replaced with 8oG. Our goal is to identify differences in electrostatic potential that might be relevant for enzymatic recognition of the damaged DNA. For this study, we chose the 5′-TGT-3′ intact

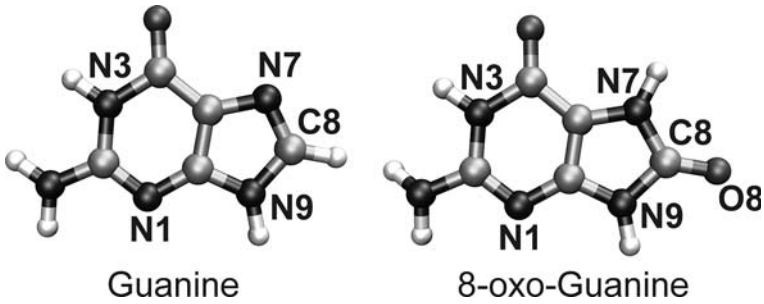

Fig. 1 Guanine and 8-oxo-guanine and atom numbering

fragment of DNA (fragment containing three nucleic base pairs, the complementary strand is 5′-ACA-3′) and the corresponding fragment containing 8oG in the place of G.

The electrostatic potential around DNA molecule is nonuniform as the molecule contains many polar groups specifically arranged in space. The analysis of electrostatic potential in three dimensions might be a very complex task. However, most of the important interactions take place near the surface of DNA. Hence, we will focus our analysis on the values of the electrostatic potential at the "molecular surface". A definition of molecular surface will be given in Sect. 2.2.2.

For the purpose of our study, we will develop and implement a cylinder projection [7–10] of the electrostatic potential, in which the values of the electrostatic potential at the molecular surface are projected onto a simpler surface. This technique is sometimes called "gnomonic projection". In our case, we project the electrostatic potential from the complicated molecular surface of DNA onto the walls of a cylinder. The resulting 2D electrostatic maps of intact and damaged DNA are then analyzed. The main features resulting from the replacement of G with 8oG are reorganizations of the countercations and phosphate groups.

2 Methods

2.1 Molecular structure and introduction of DNA lesions

To obtain the structure of intact and damaged DNA fragments, we use the same approach as described before [11]. From the starting molecule, the 5′-CTAGTTGTTCCC-3′ DNA dodecamer (Fig. S-1) described by Arnott et al. [12], we cut a 5′-TGT-3′ fragment (a trimer) containing three nucleic base pairs. To limit the size of the system, the phosphate groups were removed from the 5′ and 3′ ends and the strands were saturated with OH groups. The sodium countercations were placed at each of the four phosphate groups.

The resulting structure was a starting point for DFT optimizations using a B3LYP exchange-correlation functional [13–15]. The atoms of the top and bottom nucleic acid base pairs where fixed in space during the optimization to eliminate the unphysical "surface" effects related to a "cluster model" of DNA that we use in our study. The 6-31G** basis set was used for all geometrically optimized atoms and 6-31G basis set for the geometrically fixed atoms. In the next step, we introduced a lesion. The guanine of the intact 5′-TGT-3′ trimer was replaced with 8oG by changing H at the position 8 into oxygen and adding a hydrogen atom to N7. The initial interatomic distances and angles for 8oG in the DNA fragment were the same as those resulting from the B3LYP/6-31G** optimization for the isolated 8oG. The resulting DNA trimer with 8oG was optimized at the B3LYP/6-31G** level, and again the top and bottom pairs of nucleic acid bases were fixed in space. For the optimized geometries of the fragments of intact and damaged DNA, we calculated net atomic charges using the ESP method [16,17] and the default atomic radii.[1] The charges on atoms were fitted to reproduce the electrostatic potential around the molecule. Those atomic charges are later used in our electrostatic potential analysis.

All DFT calculations were preformed using the NWChem program package [18,19] .

2.2 Cylinder projection of electrostatic potential

2.2.1 The idea of cylinder projection and introductory video

Analysis of electrostatic potential of a molecule is a complicated process. One needs to look at the potential created by charges in the 3D space around the molecule. A simplification is provided by a technique called "gnomonic projection" [20]. Here, a fragment of the DNA molecule is positioned at the center of a cylinder and the axis of the DNA is aligned with the axis of the cylinder. The shape of the cylinder matches well the structure of a short DNA fragment. The values of EP at the surface of the DNA are projected onto the wall of the cylinder. It is not necessary to project EP onto the top and bottom of the cylinder because, in the case of DNA, these areas are occupied by other layers of base pairs.

An introductory video was prepared to explain the basics of the cylinder projection approach to the analysis of electrostatic potential around DNA molecule. A MPEG-1 format video file is attached as a supplementary material.

[1] Atomic radii used for ESP calculation (Merz-Kollman scheme): H 1 Å, C 1.47 Å, N 1.4 Å, O 1.36 Å, Na 2.1 Å and P 1.8 Å

2.2.2 Definition of molecular surface

There is no unique definition of a molecular surface because electron density is given by a charge distribution. The molecular surface may be defined in various ways depending on the task. For example, it may be defined by atomic radii [21] or van der Waals radii [22] . In the case of our study, we are interested in the molecular surface that is important for enzymatic recognition. This is the area where the DNA–enzyme interactions take place. The length of a typical hydrogen bond is 1.8–2.2 Å (defined by the distance of atomic centers). On the other hand, electrostatic interaction of charged groups has a long-range character. We believe that an interesting molecular surface might be ca. 2–5 Å from centers of the outermost atoms of DNA fragments. In this study, we assumed that the molecular surface is spanned by spheres centered on atomic nuclei. The radii for the C, N, O, H, P atoms are based on covalent radii, which are additionally increased by 2 Å . The radius for Na is based on its ionic radius, also increased by 2 Å . The used radii are presented in Table 1. One may note that covalent radii are not typically used for defining intermolecular interactions and the van der Waals radii might be more suitable for this purpose. However, we initially explored different definitions of the DNA surface, setting it from 2 to 4.5 Å from atomic centers. We found out that the main features of EP were insensitive to the details of the DNA surface. As the van der Waals radii for atoms like carbon vary significantly from one compilation source to another, we decided to use covalent radii.

2.2.3 The axis of DNA

In our implementation of the gnomonic projection approach a cylinder is built around the axis of the DNA fragment. This axis could be approximated by a vector normal to the bottom nucleic acid base pair (Fig. 2a) and passing through the geometric center of this base pair. As a nucleic acid base pair is not perfectly planar, we approximate the axis of DNA by a vector **z** (Fig. 2b) which is a cross-product of vectors connecting atoms N9 and N4 for adenine (vector **b**, Fig. 2b) and N1 of thymine with N4 of adenine (vector **a**, Fig. 2b). This approximate axis of the DNA fragment goes through a point in the middle of the line connecting N1 of thymine with N9 of adenine (axis z, Fig. 2c). Figure S-2 shows the resulting z axis in the DNA trimer. We tested the proposed construction for different fragments of DNA and in all cases the resulting z axis was meaningful.

2.2.4 Points on the molecular surface

First, equally distributed points on the cylinder wall were selected. It is done in two loops:

(a) Over the height of the cylinder along the z axis (Fig. 3),
(b) Over the angle α in the xy plane (Fig. 3)

For each step in height (along the z axis), the **R** vector (radius of the cylinder[2]) is rotated around the z axis by an angle α

[2] Radius of the cylinder was set to 20 Å

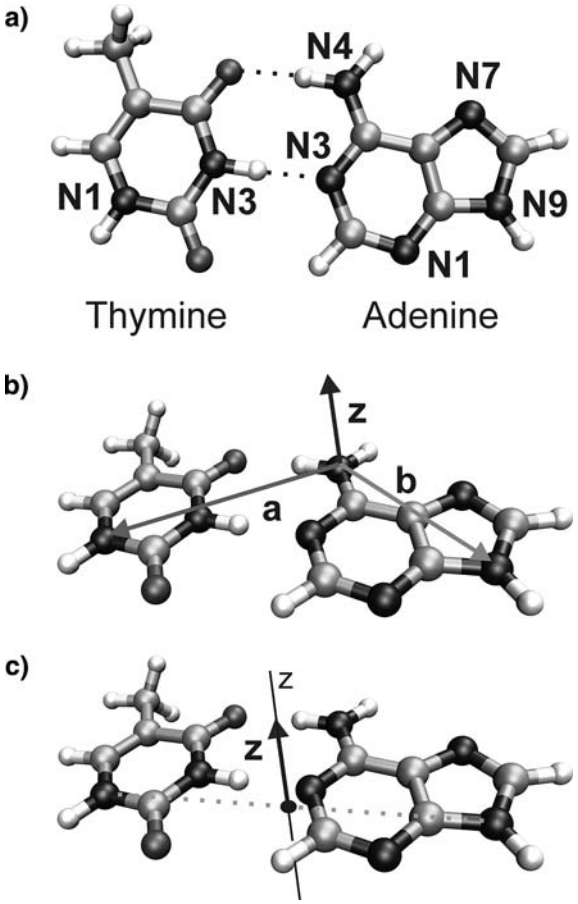

Fig. 2 Axis of DNA (axis z) approximated by a vector **z**, which is normal to the bottom nucleic acid base pair: **a** Bottom nucleic acid base pair of the DNA trimer – A-T pair and atom numbering; **b** Vector **z** – a cross product of vectors **a** and **b**; **c** Axis z, defined by the vector **z** and going through the middle of a line connecting N1 of thymine and N9 of adenine

and the resulting point on the cylinder is recorded (Fig. S-3). Each selected point on the cylinder defines a point on the DNA surface (Fig. S-4). We search for this point along **R** and passing through the preselected point on the cylinder. The outermost point on this line, $\mathbf{R}'$ (Fig. 3), for which the distance from any atom is smaller than $r_{\text{atom}}+2$Å, is the DNA surface point (r_{atom} is an atomic radius defined in Table 1). Finally, EP is calculated at each point of the DNA surface (see Sect. 2.2.5).

The final electrostatic potential map consists typically of 72000 points. The angular coordinate was scanned from 0 ° to 359 ° with a step of 1 °. The z coordinate was scanned with 200 steps of 0.05 Å each. The starting point of the z coordinate scan was set to 2Å below the bottom A-T base pair.

2.2.5 Electrostatic potential on the DNA surface and its 2D map

At each point on the molecular surface, the electrostatic potential is calculated as a sum over contributions from all atoms:

Table 1 Covalent radii for H, N, C, O, P, and ionic radius of Na (in Å)

Element	H	C	N	O	P	Na
Radius	0.37 [21]	0.77 [21]	0.74 [21]	0.74 [21]	1.10 [21]	1.02 [23]

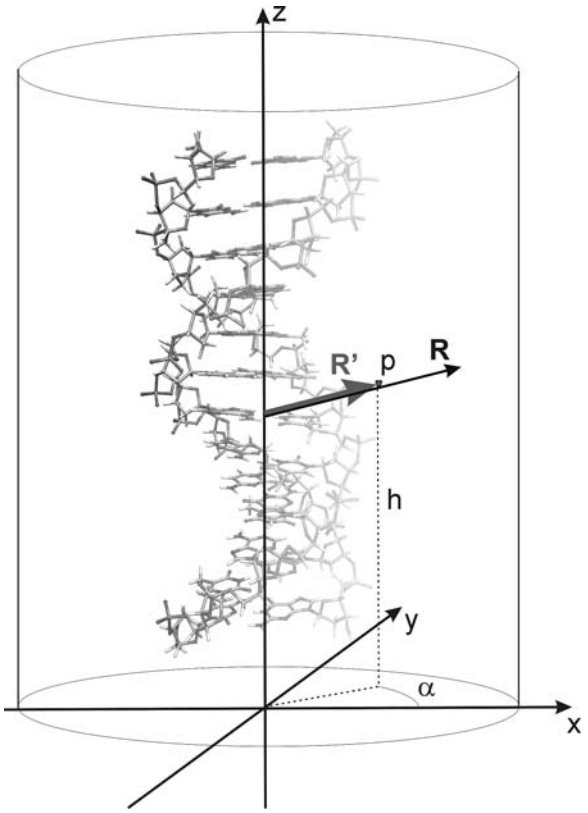

Fig. 3 Details of cylinder projection

$$\mathrm{EP}(\mathbf{p}) = \sum_{1}^{n} \frac{q_n}{|\mathbf{p} - \mathbf{r}_n|}, \tag{1}$$

where n is the total number of atoms, q_n the charge of the nth atom, and $\mathbf{r}_n$ the position of nth atom.

The final electrostatic potential 2D map is formed from the values of EP determined at the molecular surface (Fig. 5a b). The angle α and the z coordinate of each point are displayed on the horizontal and vertical axes, respectively. The color is assigned according to the value of the electrostatic potential. Red and blue points have positive and negative values of EP, respectively.

The resulting EP maps can be analyzed together with the pictures of molecules and the accompanying molecular surfaces.

2.2.6 Software

The cylinder projection of electrostatic potential is done with the in-house program EPproj written in C. The electrostatic potential maps are generated using the FreeImage library (http://freeimage.sourceforge.net) . The introductory video was prepared with additional C/OpenGL routines to the EPproj program and final processing was done with the MS MovieMaker.[3]

3 Results

First, the geometrical differences of the intact and damaged DNA fragments were analyzed. As both fragments had the same top and bottom nucleic acid base pairs fixed in space during the geometry optimization, it is possible to superimpose those pairs and compare the differences in the remaining molecular part (Figs. 4, S-5). To clarify the picture, the top and bottom base pairs were removed.

The geometrical differences of the DNA fragments containing G and 8oG are limited to a strand with the lesion. The 8oG is slightly displaced in the direction of the major groove in comparison with the position of G in the intact strand. Some reorganization of the phosphate group with a sodium countercation next to the lesion might also be observed. Those atoms are moved along the long axis of DNA because of the repulsive interaction between the negatively polarized O8 in 8oG and a negatively charged phosphate group.

The cylinder projection of EP around the DNA fragments containing G and 8oG shows multiple features (Figs. 5, S-6, S-7). The EP maps are analyzed by comparing them with pictures of the DNA trimers with probed surface points (Fig. S-4). The most important features are marked on Figs S-6 and S-7. The most distinctive features are sodium countercations that are represented by four big red spots of a positive electrostatic potential. The sugar-phosphate backbones are represented by two elongated shapes of a neutral potential. The minor and major grooves might be seen between the two strands. The grooves are characterized by a negative potential. The guanine base might be associated with a big spot of a negative potential in the major groove. This negative potential is coming from a nitrogen N7 and an oxygen O4 of guanine.

At the first glance, the EP map of the DNA fragment with 8oG looks very similar to the EP map of the intact fragment. The sodium countercations, strands, and grooves might be identified in both cases. The intensity of colors, reflecting the values of EP, is very similar except of the middle part of the plot, suggesting that the lesion did not affect the DNA structure much . The features coming from 8oG are displayed in the major groove, where previously a negative potential was coming from the intact guanine. A spot in the middle of the major groove, which corresponds to a positive electrostatic

[3] MS MovieMaker is a part of MS WindowsXP operating system

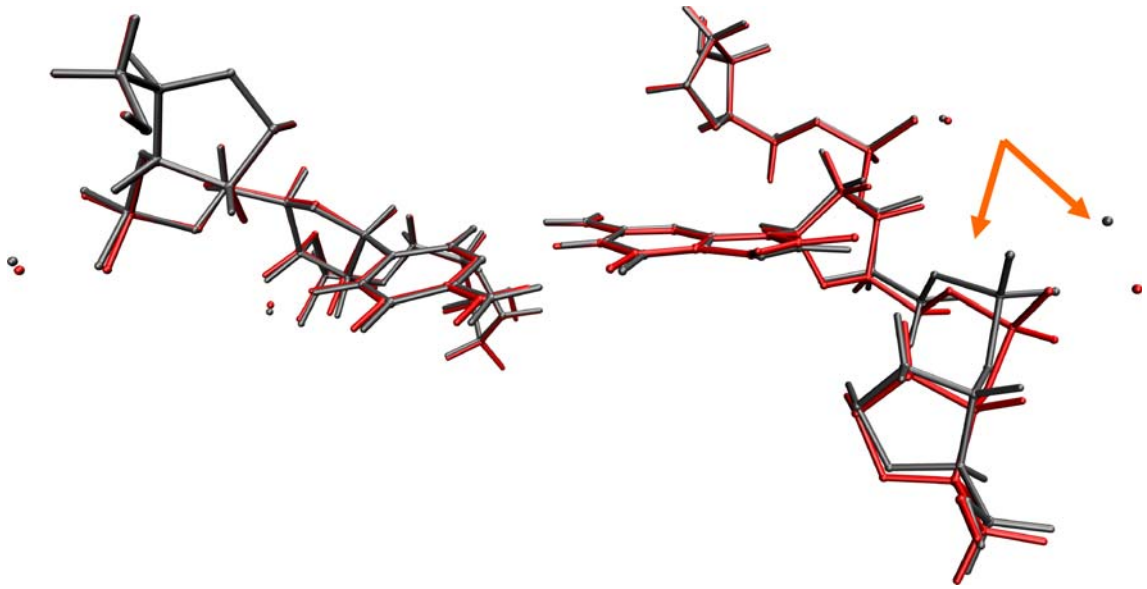

Fig. 4 The superimposed intact *(gray)* and damaged *(red)* DNA trimers show differences in geometry. Top and bottom base pairs were removed to clarify the picture. *Arrows* mark a small relaxation of the damaged strand next to the lesion and a reorganization of sodium countercations

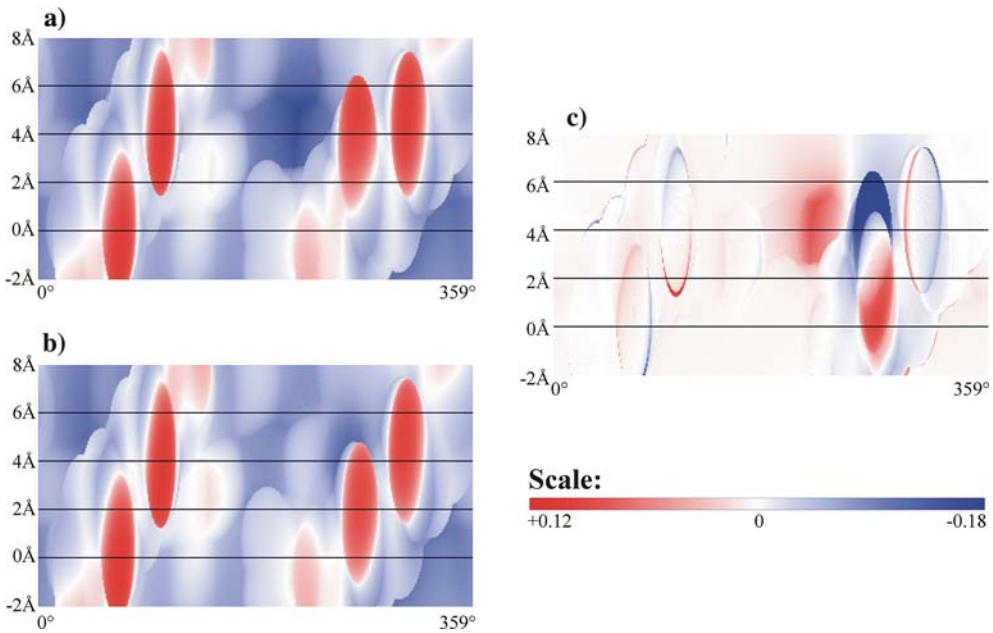

Fig. 5 Electrostatic potential maps of intact **a** and damaged **b** DNA trimers together with a difference map **c**. Angular coordinate α is placed on horizontal axis and the height h is on the vertical axis with zero set to the bottom AT pair

potential, is correlated with a hydrogen attached to N7 of 8oG.

A plot showing the difference in the EP maps for the damaged and intact DNA is presented in Fig. 5c. The differences in electrostatic potential are limited to the damaged site. The sodium countercation is moved along the long axis of DNA. The features of positive electrostatic potential coming from the N7 hydrogen of 8oG disrupt a negative potential in the major groove.

4 Conclusions

An intact 5′-TGT-3′ fragment of DNA and its counterpart with G replaced with 8oG (5′′-T8oGT-3′) were studied using the B3LYP/6–31G** method. The geometries of 5′-TGT-3′ and 5′-T8oGT-3′ were optimized with a constraint of the fixed top and bottom base pairs. The electrostatic potential around the DNA fragments was studied using the cylinder projection technique. The values of electrostatic potential at the

molecular surfaces were projected onto the walls of cylinders surrounding the DNA fragments. The resulting maps of electrostatic potential with accompanying geometries of intact and damaged DNA fragments were analyzed and the results are summarized in the following points:

1. It was found that the presence of the 8oG lesion distorts the geometry mainly at the damaged site. The relaxation of the complementary strand is minimal.
2. The damaged nucleic acid base is slightly displaced in the direction of the major groove in comparison with the position of the corresponding undamaged base in the intact DNA fragment.
3. A reorganization of counteractions together with the neighboring phosphate groups is a distinct feature of the 8-oxoguanine lesion. The relaxation of charged particles along the axis of the DNA fragment is clearly reflected in the electrostatic potential maps.
4. A negative electrostatic potential character of the major groove is disrupted by the occurrence of 8oG. A positive electrostatic potential, which results from a hydrogen atom connected to N7 of 8oG, is manifested in the EP map.

Our future study will focus on the analysis of the molecular shape of the damaged and undamaged DNA fragments. Molecular dynamics simulations will be performed to find a correlation between the distribution of countercations and the findings presented here.

Acknowledgements The authors would like to thank Maciej Sobczak for his helpful comments on the source code of the cylinder projection program. Helpful discussions with John Miller and Michel Dupuis are gratefully acknowledged.

This research was supported by the US DOE, Office of Biological and Environmental Research and Polish State Committee for Scientific Research (KBN) Grant DS/8221-4-0140-6. This research was performed using the Molecular Sciences Computational Facility (MSCF) in Environmental Molecular Sciences Laboratory (EMSL). EMSL is a national scientific user facility sponsored by the US DOE, OBER, and located at PNNL. Computing resources were available through a Computational Grand Challenge Application grant.

References

1. Lutz WK (1990) Mutat Res 238:287
2. Ames BN (1989) Mutat Res 214:41
3. Ames BN (1989) Environ Mol Mutagen 14:66
4. Ames BN, Gold LS (1991) Mutat Res 250:3
5. Lindahl T (1993) Nature 362:709
6. Fromme JC, Banerjee A, Huang SJ, Verdine GL (2004) Nature 427:652
7. Van Geerestein VJ, Perry NC, Grootenhuis PG, Haasnoot CAG (1990) Tetrahedron Comput Methodol 3:595
8. Perry NC, van Geerestein VJ J Chem Inf And Comp Sci 32:607
9. Chau P-L, Dean PM (1987) J Mol Graph 5:97
10. Blaney FE, Edge C, Phippen RW (1995) J Mol Graph 13:165
11. Miller JH, Aceves-Gaona A, Ernst MB, Harańczyk M, Gutowski M, Vorpagel ER, Dupuis M (2005) Rad Res 164:582
12. Arnott S, Chandrasekaran R, Birdsall DL, Leslie AGW, Ratliff RL (1980) Nature 283:743
13. Becke AD (1988) Phys Rev A 38:3098
14. Becke AD (1993) J Chem Phys 98:5648
15. Lee C, Yang W, Paar RG (1988) Phys Rev B 37:785
16. Besler BH, Merz KM Jr, Kollman PA (1990) J Comp Chem 11:431
17. Singh UC, Kollman PA (1984) J Comp Chem 5:129
18. Straatsma TP, Apra E, Windus TL, Bylaska EJ, de Jong W, Hirata S, Valiev M, Hackler M, Pollack L, Harrison R, Dupuis M, Smith DMA, Nieplocha J, Tipparaju V, Krishnan M, Auer AA, Brown E, Cisneros G, Fann G, Früchtl H, Garza J, Hirao K, Kendall R, Nichols J, Tsemekhman K, Wolinski K, Anchell J, Bernholdt D, Borowski P, Clark T, Clerc D, Dachsel H, Deegan M, Dyall K, Elwood D, Glendening E, Gutowski M, Hess A, Jaffe J, Johnson B, Ju J, Kobayashi R, Kutteh R, Lin Z, Littlefield R, Long X, Meng B, Nakajima T, Niu S, Rosing M, Sandrone G, Stave M, Taylor H, Thomas G, van Lenthe J, Wong A, Zhang Z (2004) NWChem, a computational chemistry package for parallel computers, version 4. Pacific Northwest National Laboratory, Richland
19. Kendall RA, Aprà E, Bernholdt DE, Bylaska EJ, Dupuis M, Fann GI, Harrison RJ, Ju J, Nichols JA, Nieplocha J, Straatsma TP, Windus TL, Wong AT (2000) Comput Phys Commun 128:260
20. Leach AR, Villet VJ (2003) An introduction to chemoinformatics. Kluwer Academic,Dordrecht, p118
21. Wells AF (1993) Structural inorganic chemistry 5/E (polish translation). Wydawnictwa Naukowo-Techniczne 1993
22. Bondi A (1964) J Phys Chem 68:441
23. Shriver DF, Atkins PW, Langford CH (1995) Inorganic chemistry 2nd edn. Oxford University Press, Oxford, p35